Gamma Ray Spectroscopy For Neutrino Experiments

Hallie Knorr
Bowling Green State University, Department of Physics and Astronomy, Ohio, 43403, USA
(Dated: July 2024)

When studying neutrinos and dark matter, researchers must minimize background events coming from unrelated processes. One source of background comes from naturally occurring long-lived radioisotopes in experiment materials. To address this, High Purity Germanium (HPGe) detectors are used to screen materials for neutrino experiments using gamma ray spectroscopy. HPGe detectors are excellent radiation detection devices, due to their high energy resolution and intrinsic purity. The data from these detectors provide detailed information about the energy and intensity of gamma rays, allowing us to quantify different radioactive sources present in samples. In this paper I will discuss the performance of two HPGe detectors I operated as part of my research experience at Virginia Tech. In particular, I will discuss the experimental setup, calibration of the detector energy response, and measurement of detection efficiency with point calibration sources.

I. INTRODUCTION

High Purity Germanium (HPGe) detectors were first introduced in the 1970s [1]. These detectors have been used by many researchers, especially those interested in neutrinos and dark matter. HPGe detectors are semiconductor diodes that measure gamma-ray energies in high resolution. They convert these gamma-rays into electrical impulses that are used to idenitfy the energy and intensity of the gamma-rays [2]. They display their results in gamma and x-ray spectroscopy. The development of these semiconductors has evolved for more than fifty years. These types of detectors started out as lithium-drifted germanium (Ge(Li)) and lithium-drifted silicon (Si(Li)) [3]. Over time, these detectors progressed to the usage of high purity germanium. Using high purity germanium in these semiconductors is more efficient than using silicon. This is due to germanium having a higher atomic number and therefore having a lower energy cost for creating electron-hole pairs [4]. With these germanium detectors they allow for high resolution in the upper gamma energy levels. This is why HPGe detectors are popular to use when identifying radioisotopes and viewing high energy levels on a spectroscopy. Figure 1 shows the spectroscopy of two HPGe detectors and the range of gamma-energies in keV.

HPGe detectors have many great features compared to other semiconductor detectors. One of the main features of these detectors is having high energy resolution. This allows the HPGe detectors to precisely distinguish and measure the energies of different gamma rays. In the spectra produced by these detectors, the full energy peaks are very sharp [2]. Having these sharp peaks helps to accurately identify radioisotopes. This one feature alone makes these detectors more effective when detecting and quantifying gamma radiation. Figure 2 showcases the sharp peaks HPGe detectors can produce on a spectroscopy.

Due to germanium's low band gap, HPGe detectors must be cooled down to very low temperatures in order to maximize their efficiency. Cooling down the detectors reduces thermal excitation's of valence electrons [5]. This allows the detectors to better measure the energy that the gamma rays give to an electron in order to cross the band gap and reach the conduction band [5]. Liquid nitrogen is used to cool down these detectors and keep them cool during the data taking process. With liquid nitrogen, the detectors stay cool at around 77 Kelvin. Special insulated tubing is used to transfer the liquid nitrogen into cryostat tanks. This process was done weekly and it took around thirty minutes to completely fill up a single cryostat tank. Figure 3 shows what the liquid nitrogen tanks looked like.

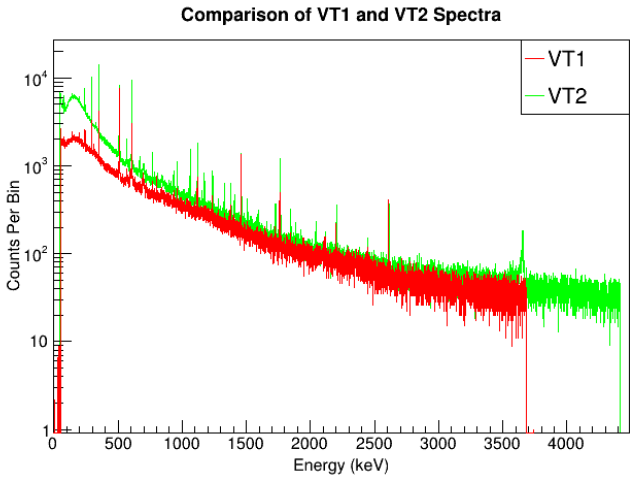

FIG. 1. *Two sets of histograms from two HPGe Detectors. This spectroscopy consists of 14 combined days of data. The max energy level for detector 1 is approximately 3700keV and for detector 2 it is approximately 5000keV.*

II. HPGE DETECTOR ORIENTATIONS

To house this liquid nitrogen, cryostats are incorporated in with the detectors. Cryostats have vacuum

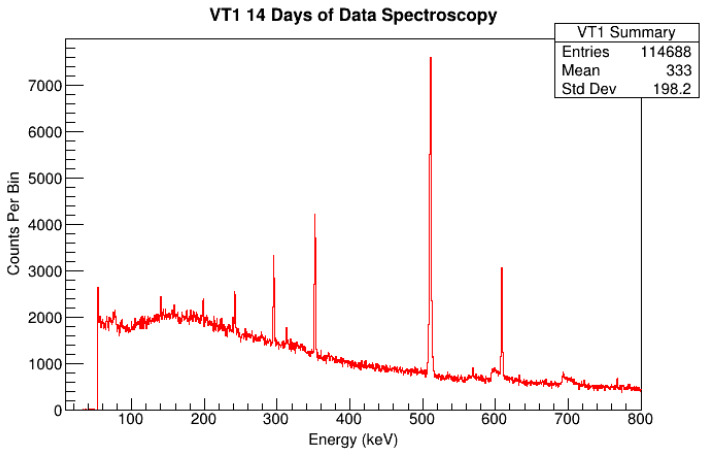

FIG. 2. *Gamma Ray spectroscopy from HPGe detector 1. This spectroscopy consists of 14 combined days of data.*

FIG. 3. *The is an image of one of the liquid nitrogen tanks used throughout our research. One tank held about 240 liters*

chambers that accommodate the detector element and a dewar all in one system. These dewars have insulated double wall vacuums that are used for the liquid nitrogen cryogen [5]. In most HPGe detectors the detector portion is kept in place by an anti-microphonic stabilizer which allows the detector element to be thermally connected through a copper cold finger [5]. This cold finger will transfer the heat from the detector element all the way down to the liquid nitrogen tank. In order to avoid the attention of lower energy photons, the detectors holder and the cap around this holder are very thin and made of aluminum. [5]. Figure 4 shows what these detector elements look like.

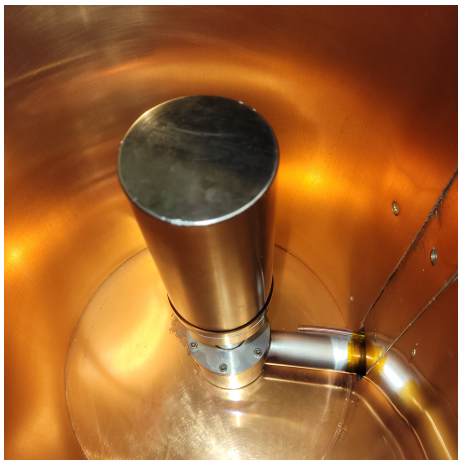

FIG. 4. *An image of VT1's detector element*

Now in order to get the ideal background data from these HPGe detectors, the detector portion itself should be encased with specific shielding. Looking inside the shielding of these detectors there is a thin copper barrier followed by a thick layer of lead. Figure 5 shows an example of the proportions of this shielding. Lead has a high atomic number (82), with this it is great for blocking environmental radiation. However, lead itself produces radiation, so the thin layer of copper is there to protect the detector element. These two materials help the detectors measure better results in our background data since they create an inner environment for the detectors. Figure 5 shows the thickness of the shielding for the detectors.

FIG. 5. *This image shows the thick lead shielding around the copper barrier that surrounds VT1's detector element.*

For this research, The comparison of two different types of HPGe detectors will take place using their background data and analyzing their efficiencies. The two HPGe detectors are labeled as VT1 and VT2. These two detectors have different orientations and very different

looks, but they both are equipped with 30-liter dewars. The first HPGe detector named VT1 is an Integral cryostat, while the second HPGe detector named VT2 is a dipstick cryostat. VT1 has a more sophisticated look to it as the shielding around the detector element was highly developed compared to VT2. VT1 has a cylindrical shape of shielding surrounding the detector element, while VT2 has a cubical shape of shielding.

A. VT1

HPGe detector VT1 has the orientation called Integral Cryostat. This cryostat has a common vacuum chamber and the detector dewar cannot be separated without breaking the vacuum [5]. Figure 6 shows a diagram for an integral cryostat. VT1 is horizontally orientated and the shielding around the detector chamber is cylindrical. The images in figures 7 and 8 show the inside and outside of VT1.

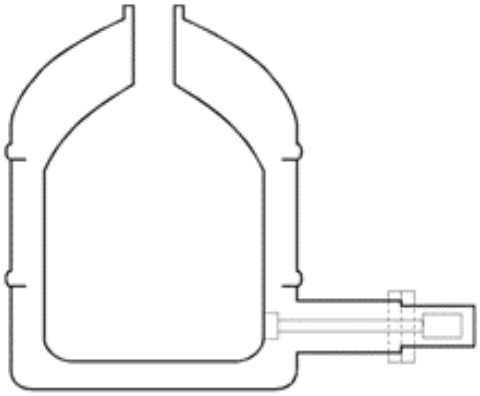

FIG. 6. *A diagram of an integral cryostat. This is the orientation that detector VT1 displayed. Image sourced from Mirion Technologies [5].*

FIG. 7. *Outside of VT1. The dewar is located on the right with the detector chamber in its shielding connected to the left*

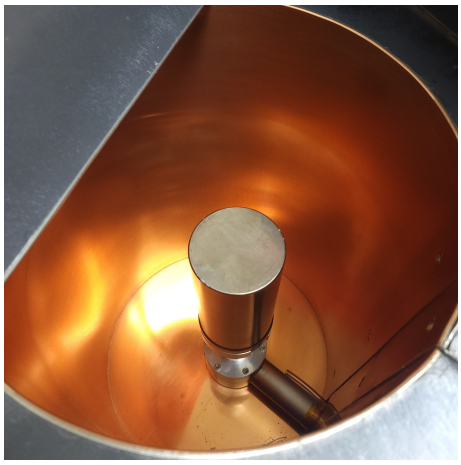

FIG. 8. *Inside of VT1. Centered in the middle of the cylindrical chamber is the detector element.*

B. VT2

HPGe detector VT2 has the orientation called Dipstick cryostat. This cryostat has a long dipstick like pole that is inserted into the dewar. At the end of this pole is a copper cold-finger. This cold finger's purpose is to cool the detector element using the liquid nitrogen it's dipped in [5]. One of the main differences with this type of cryostat is it has separate vacuums for the dewar and detector element. This vacuum system has absorber material which helps maintain a better vacuum [5]. Figure 9 shows a diagram setup for a dipstick cryostat. VT2 is vertically orientated and the shielding around the detector chamber is cubical. The images in figures 10 and 11 show the inside and outside of VT2.

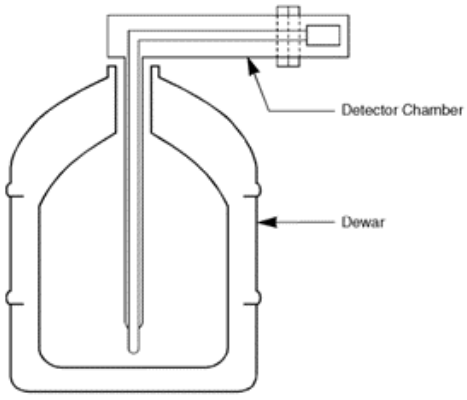

FIG. 9. *A diagram of a dipstick cryostat. Although VT2 has a vertical detector chamber orientation, this is a good representation of how the dipstick fits into the dewar. Image sourced from Mirion Technologies [5]*

FIG. 10. *Outside of VT2. The dewar is located on the bottom with the detector chamber in its shielding connected above*

FIG. 11. *Inside of VT2. Here we can see the detector chamber and a radioactive collaboration placed inside.*

III. OPTIMIZATION

For collecting data from the HPGe detectors a 5-kV radiation detector bias supply was used along with two spectroscopy amplifiers, a digital gamma ray spectrometer and Maestro software. With these machines and systems, data was able to be collected over extended periods. The 5-kV radiation detector bias supply used was the model 660 from the company ORTEC. This ORTEC model is equipped with two completely independent 0-5kV supplies. On the detector bias supply, A was set for VT1 and B was set for VT2. The spectroscopy amplifiers used were the models 672 and 671 from ORTEC [6] [7]. VT1 was connected to Model 672 and VT2 was connected to Model 671. The digital gamma ray spectrometer used was the EASY-MCA from ORTEC as well [8]. Figure 15 in Appendix VIII shows an example of the setup for wiring all these devices together with a HPGe detector.

From the amplifiers, data was taken from the back for both VT1 and VT2.The data collected do not differ when taking the output from the back compared to the front. For all the intricate settings on the amplifiers we optimized each detector using the ORTEC manuals written for each device. Most of the settings were kept the same for both detectors except for the gain and high voltage levels. For both detectors the input was set to Normal and negative, the PZ set to auto, and the shaping time set at 3 microseconds. These settings were chosen because they gave the highest resolutions and the optimal range of gamma energies for the detectors.

For VT1 the fine gain was set to 1.4 and the coarse gain to 10. To get the total gain, you multiply these two numbers together. With this VT1 had 14 total gain. For VT2 the fine gain was set to 0.5 and the coarse gain to 50, so the total gain was 25. Now, on the detector bias supply the high voltage was set to different levels. The 5-kV radiation detector bias supply manual did provide recommend high voltage levels. For VT1 the voltage was set to 4100kV and for VT2 the voltage was set to 5000kV. All these settings gave both detectors the best optimization.

IV. DATA COLLECTION

To collect the background data from these HPGe detectors a program called Maestro was implemented. This Maestro software is a graphical user interface to the data acquisition for VT1 and VT2 [9]. This software develops data from the HPGe detectors and creates digital gamma ray spectra. Job files were used to start and control the data taking process. These job files controlled how long the HPGe detectors would run for and where they were saved. Separate job files were created for each detector. This allowed both detectors to run and collect data at the same time. To reduce the impact of interruptions in the data taking process, the job files looped once a day. That way the data would be saved each day, so if something were to happen and the job file quit, there would still be data from the previous days. For both detectors 14 days of data was taken. Figure 12 shows the set up for the bias supply and amplifiers.

A. Calibration

Before collecting any data, it is very important to calibrate the detectors. This was successfully done by using calibration sources. Calibration sources are small samples of radioactive substances with common decay radiation energy's that are easily identifiable on a gamma ray spectroscopy. Figure 13 displays what these sources look like from Virginia Tech. The easiest and most accurate

FIG. 12. *An image of the 5-kV radiation detector bias supply (left), Model 672 spectroscopy amplifier (middle), and Model 671 spectroscopy amplifier (right)*

source used was Co-60 (cobalt). Cobalt's decay radiation for gamma and x-rays has two very distinct energy levels. These levels are at 1173keV and 1332keV. They both have a little over 99% chance of being detected in the HPGe detectors according to the National Nuclear Data Center [10]. This high percentage is what makes these energies good for calibration.

FIG. 13. *Radioactive sample Co-60 used for calibration.*

The calibration process starts by placing the radioactive sample inside the HPGe detector. These samples were specifically placed right on top of the detector element. You can revert back to figure 11 to see a sample placed inside VT2. Once the sample is placed, the detector is closed up so the copper and lead shielding can be effective. Once everything is secure, a Maestro run can be started. This allows the detector to run, and the gamma ray spectroscopy begins to form. For calibration, the detectors run for a couple of hours. Once the detectors were done running, tools from the Maestro software calibrated the collected data. Calibration is done by finding the identifiable peaks. When using Co-60, the peaks at 1173keV and 1332keV were the ones used. Once these peaks were identified the software could tell the detector to remember where these peaks lied. With this the keV energies are shifted into the correct spots. After this is done all of the future data collected will be correctly calibrated. Figure 16 in Appendix VIII shows the Maestro program after completing a calibration run with cobalt.

V. DATA ANALYSIS

The data collected from the two HPGe detectors provided many useful spectra that helped show the characterizations of VT1 and VT2. In order to analyze the collected data, C++ code was utilized to combine data and create histogram graphs. Referring back to figure 1, this graph portrays the combination of two histograms and compares the overall data between VT1 and VT2. In the graphs created from the collected data, histograms were used to better analyze the gamma ray peaks in the spectra and Gaussian curves were fitted to these peaks. All histograms were developed with bin widths of 100 and have 114,688 entries. This is due to having 14 days of data for each detector. We completed four Gaussian curve graphs for each detector. These graph are presented in Appendix VIII as figures 17-24.

Each of these graphs have a summary box about the Gaussian curve distribution. This summary box includes the number of entries, the mean value, the standard deviation, x^2, and 4 different parameters for the Gaussian curve. Parameter 0 (N) is the value of the number of counts per bin at the top of the Gaussian curve. Parameter 1 (μ) is the energy level in keV where the middle of the Gaussian curve lands. Parameter 2 (σ) is the half width at the half maximum point on the Gaussian curve. Parameter 3 is the flat background for the Gaussian curves. Tables 1 and 2 show all the data from these graphs.

TABLE I. VT1's data measured from the Gaussian parameters.

Peak(keV)	Counts(N)	Energy(μ)	HWHM(σ)	Background
Pb-214(352)	5,661	352 keV	0.705 keV	1179
Bi-214(609)	4,211	609 keV	0.747 keV	761
K-40(1460)	3,590	1458 keV	0.982 keV	184
Ti-208(2615)	1,217	2608 keV	1.345 keV	50

TABLE II. VT2's data measured from the Gaussian parameters.

Peak(keV)	Counts(N)	Energy(μ)	HWHM(σ)	Background
Pb-214(352)	22,399	351 keV	0.746 keV	1179
Bi-214(609)	17,415	609 keV	0.823 keV	761
K-40(1460)	3,495	1460 keV	1.221 keV	184
Ti-208(2615)	1,189	2614 keV	1.712 keV	50

A. Efficiency Calibration

It's important to know the efficiency of the detectors to be able to interpret the data. The efficiency of each detector was measured after collecting all of the initial data. The efficiency of a HPGe detector at a particular energy can be measured by taking the ratio of the number of gamma rays observed over the number expected. This ratio is shown as Eq. 1

$$Efficiency = N_{Observed}/N_{Emitted} \tag{1}$$

Radioactive sources were used to take efficiency calibration data for each detector. There were three different types of samples used. They were Cs-137(Cesium), Eu-152(Europium), and Na-22(Sodium). Figure 14 shows these three samples in their protective cases.

FIG. 14. *In this image we used three out of the four pictured high radioactive samples for efficiency calibration.*

For each detector, three data runs were taken, one for each sample. The duration of these runs were only twenty minutes. This is due to the samples being very active and so the detectors pick up their gamma ray energies fast. Once the six runs were completed, the yields could be measured for the specific gamma rays chosen from the sources. One gamma peak was chosen from each sample. For Cs-137, the peak 662keV was used. For Eu-152, 1408keV was used and for Na-22, 511keV was used. These peaks were chosen because they had high percentages of being detected. Figures 25-31 in Appendix VIII are the results of these efficiency calibrations. Once these yields were acquired for each detector, then the number of gamma rays expected could be calculated. The activity at any time t, $(A(t))$, follows the radioactive decay law:

$$A(t) = A_0 e^{-t/\tau} \tag{2}$$

where A_0 is the activity at production time, and τ is the mean lifetime of the decay. Tables 3 and 4 show the efficiency data for each detector. From this data VT2 can be seen as having a higher overall efficiency compared to VT1. Although the percentage of uncertainty in the detector's efficiency is approximately 5%.

TABLE III. A table of the $N_{Observed}$ values, the $N_{Emitted}$ calculated values and the measured efficiencies for VT1

Source(keV)	$N_{Observed}$	$N_{Emitted}$	Efficiency(%)
Na-22(511)	187,506	2,389,463	7.8
Cs-137(662)	92,671	2,073,699	4.5
Eu-152(1408)	23,784	1.065.242	2.2

TABLE IV. A table of the $N_{Observed}$ values, the $N_{Emitted}$ calculated values and the measured efficiencies for VT2

Source(keV)	$N_{Observed}$	$N_{Emitted}$	Efficiency(%)
Na-22(511)	209,594	2,389,463	8.8
Cs-137(662)	101,155	2,073,699	4.9
Eu-152(1408)	29,901	1.065.242	2.8

VI. RESULTS

A total number of 15 graphs were created from the data of this research. 9 of these graphs showcased a comparison between detectors VT1 and VT2. The other 6 graphs were used specifically for measuring the efficiencies at certain peaks for both detectors. Throughout all this data and analysis a few characterizations were able to be made.

For VT1, the half width at the half maximum(HWHM) was slightly smaller compared to VT2. This can be seen true throughout all of the graphs created. This means VT1 has a better overall resolution. For VT2 the number of counts per bin were mostly higher than VT1. However, VT1 had more counts per bin at the peak Ti-208(Thallium) located at 2615keV. Based on this observation VT1 has a higher counts per bin rate at higher energy levels compared to VT2. One last observation that can be made is the fact that VT1's peaks gradually began to shift over to the left on the graphs as compared to VT2. Throughout our figures

VT1 and VT2's peaks are for the most part lined up. Around the energy level 800keV, VT1's peaks begin to shift horizontally left. Unlike VT2's peaks which stay correctly aligned with the calibrated energy levels. This is especially noticeable in table 1 with the peaks located at 1460keV and 2615keV. This shift in VT1 is likely due to a nonlinear term in the calibration function, which is not handled in the Maestro software, but it could be corrected in an offline analysis.

Overall, HPGe detectors VT1 and VT2 have similar results when compared to one another. There are a few notable differences which were discussed but I would not say one detector out ranks the other. HPGe detectors are very useful tools when it comes to screening materials for neutrino experiments, and they will continue to be used by researchers in the future.

VII. ACKNOWLEDGEMENTS

The first person I would like to thank is my mentor, Professor Thomas O'Donnell. He was there with me every step of the way and guided me graciously. I would also like to thank graduate student Aaron Torres for all his help and teaching me so much. I am very grateful for the REU Virginia Tech Program for giving me this opportunity and the support from the Virginia Tech Center for Neutrino Physics. I also acknowledge support from the National Science Foundation, the Virginia Tech Physics Department and the Virginia Tech Center for Neutrino Physics.This work was made possible by the National Science Foundation under grant No.PHY-2149165.

[1] Semiconductor Detector Development, Applied Nuclear Physics Program, LBNL, https://anp.lbl.gov/semiconductor-detector-development/.

[2] The Best Choice of High Purity Germanium (HPGe) Detector, ORTEC, https://www.ortec-online.com/-/media/ametekortec/technical-papers/high-purity-germanium-detector-applications-and-technology-advancements/best-choice-high-purity-germanium-hpge-detector.pdf ().

[3] High Purity Germanium (HPGe) Radiation Detector, ORTEC, https://www.ortec-online.com/products/radiation-detectors/high-purity-germanium-hpge-radiation-detectors ().

[4] High Purity Germanium Detectors - HPGe, https://www.nuclear-power.com/nuclear-engineering/radiation-detection/semiconductor-detectors/high-purity-germanium-detectors-hpge/.

[5] Germanium Detectors User Manual, Mirion Technologies, http://www.nuclearphysicslab.com/npl/wp-content/uploads/Germanium_Detectors_Users_Manual_Rev_G_9231358G.pdf.

[6] Model 672 Spectroscopy Amplifier Operating and Service Manual, ORTEC, https://www.ortec-online.com/-/media/ametekortec/manuals/6/672-mnl.pdf.

[7] Model 671 Spectroscopy Amplifier Operating and Service Manual, ORTEC, https://www.ortec-online.com/-/media/ametekortec/manuals/6/671-mnl.pdf.

[8] Detector Bias Supply Operating and Service Manual, Mirion Technologies, https://www.ortec-online.com/-/media/ametekortec/manuals/6/660-mnl.pdf?la=en&revision=582dfa0e-b502-40f2-ab15-f8784eea58e7.

[9] MAESTR0 Multichannel Analyzer Emulation Software, ORTEC, https://www.ortec-online.com/products/software/maestro-mca.

[10] National Nuclear Data Center, https://www.nndc.bnl.gov/nudat3/.

VIII. APPENDIX

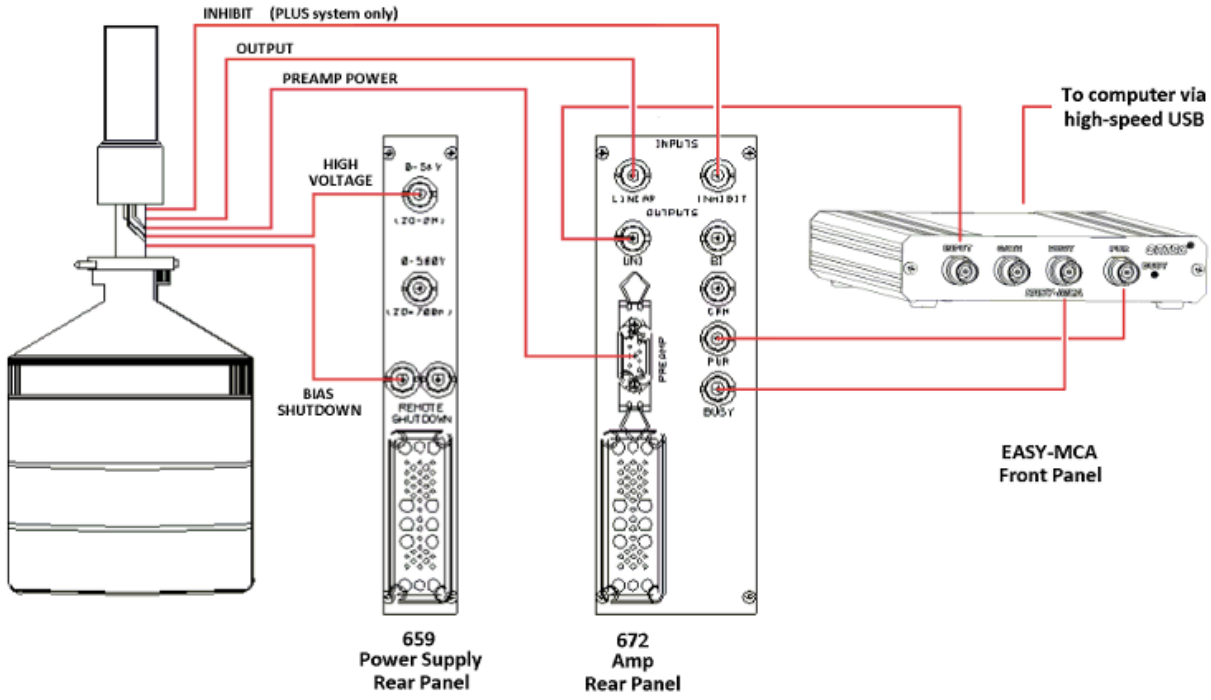

FIG. 15. *A diagram of an example setup for the wiring between a HPGe detector, a radiation detector bias supply, a spectroscopy amplifier, and a digital gamma ray spectrometer [5].*

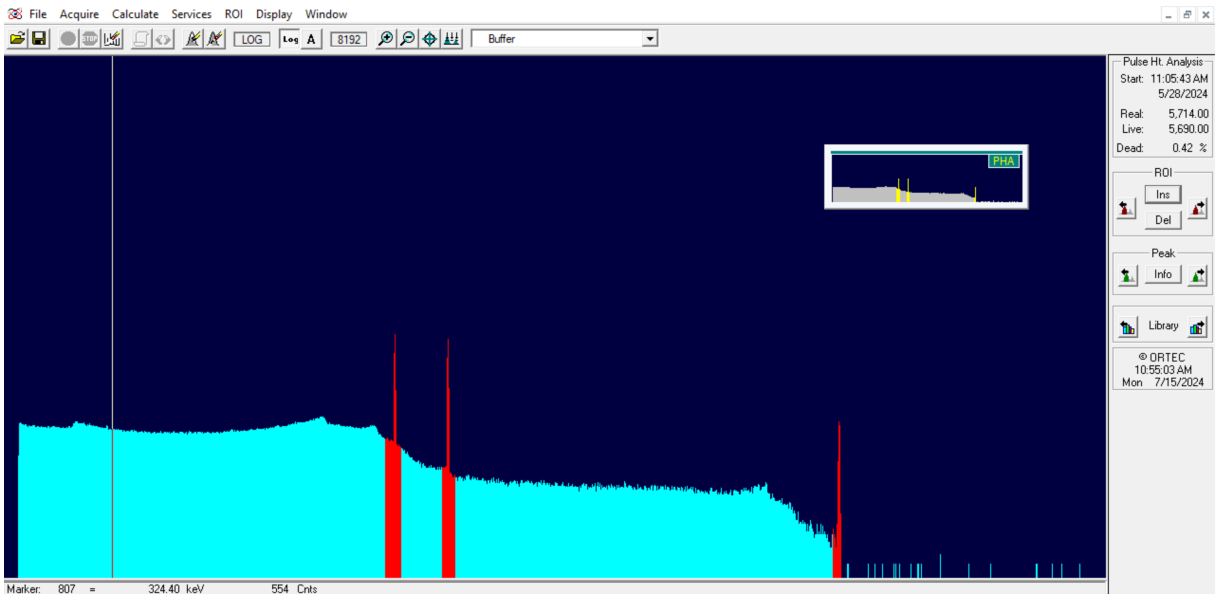

FIG. 16. *This is an image of the Maestro display. Here we can see the highlighted keV peaks of 1173 and 1332. These peaks were used to accurately calibrate both HPGe detectors.*

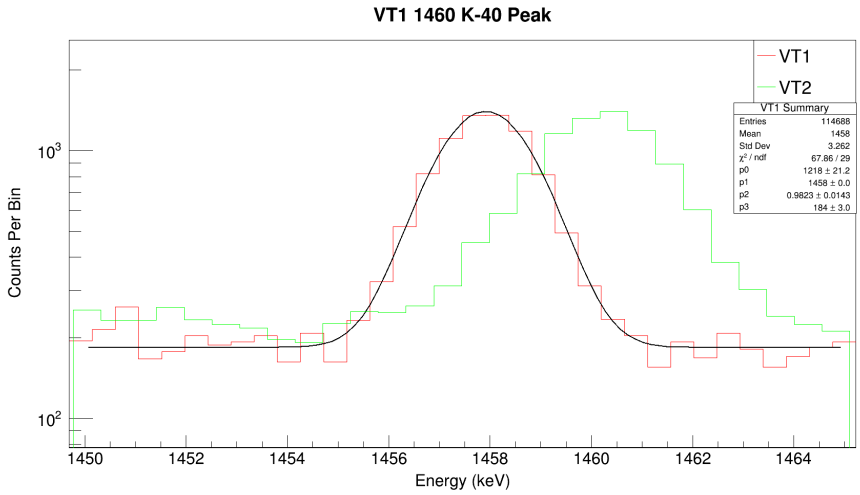

FIG. 17. *VT1's histogram of peak K-40 (Potassium) with counts per bin on the y-axis and gamma-energies on the x-axis.*

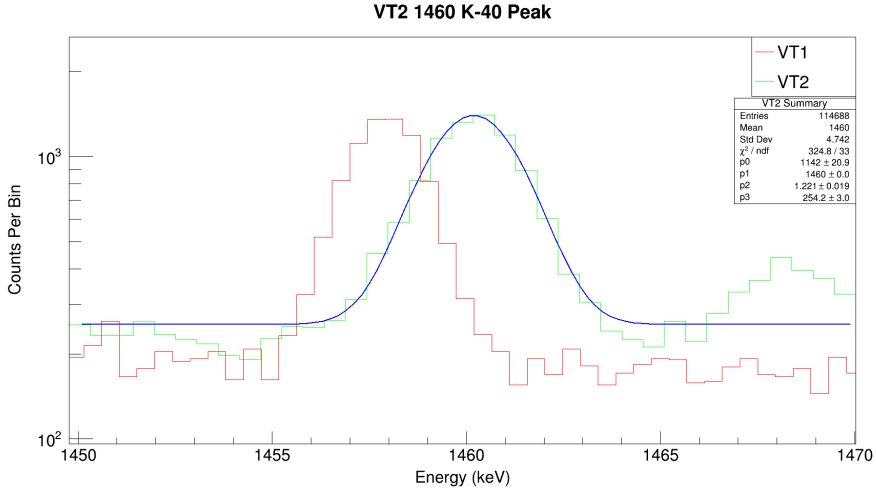

FIG. 18. *VT2's histogram of peak K-40 (Potassium) with counts per bin on the y-axis and gamma-energies on the x-axis.*

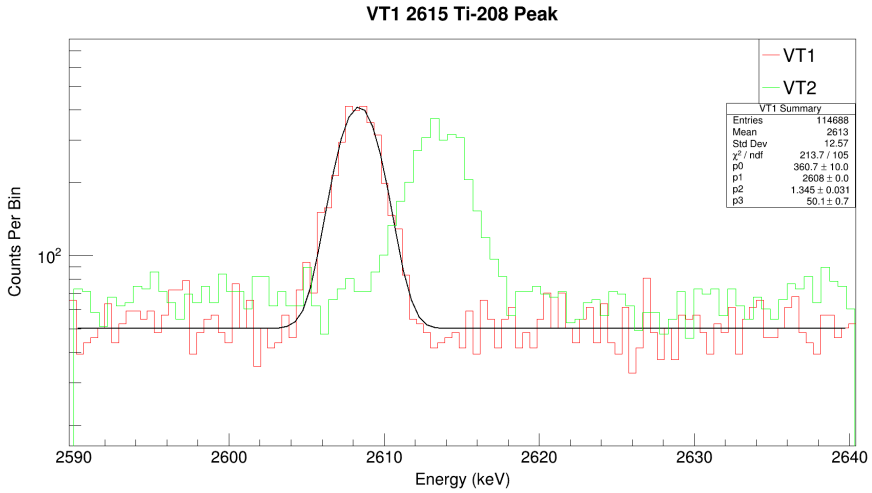

FIG. 19. *VT1's histogram of peak Ti-208 (Thallium) with counts per bin on the y-axis and gamma-energies on the x-axis.*

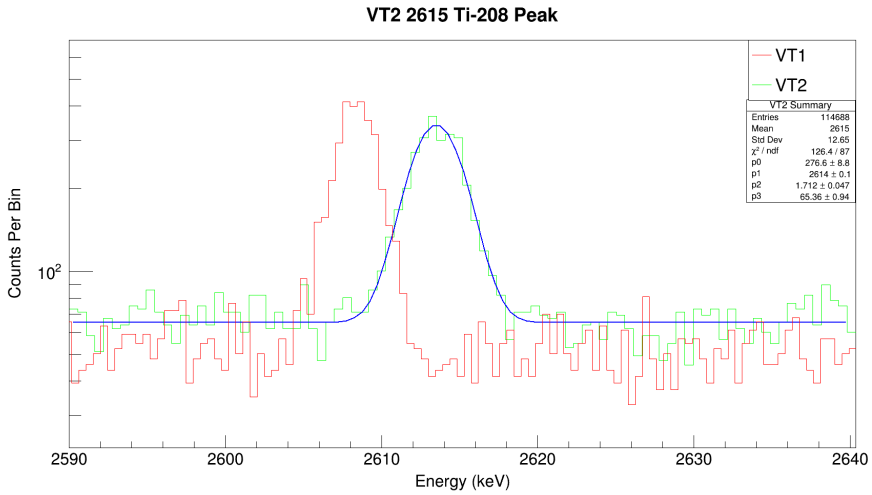

FIG. 20. *VT2's histogram of peak Ti-208 (Thallium) with counts per bin on the y-axis and gamma-energies on the x-axis.*

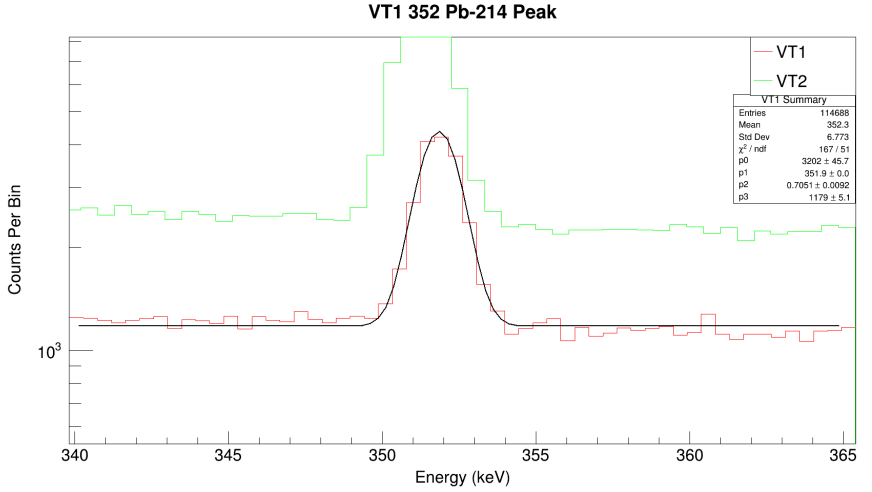

FIG. 21. *VT1's histogram of peak Pb-214 (Lead) with counts per bin on the y-axis and gamma-energies on the x-axis.*

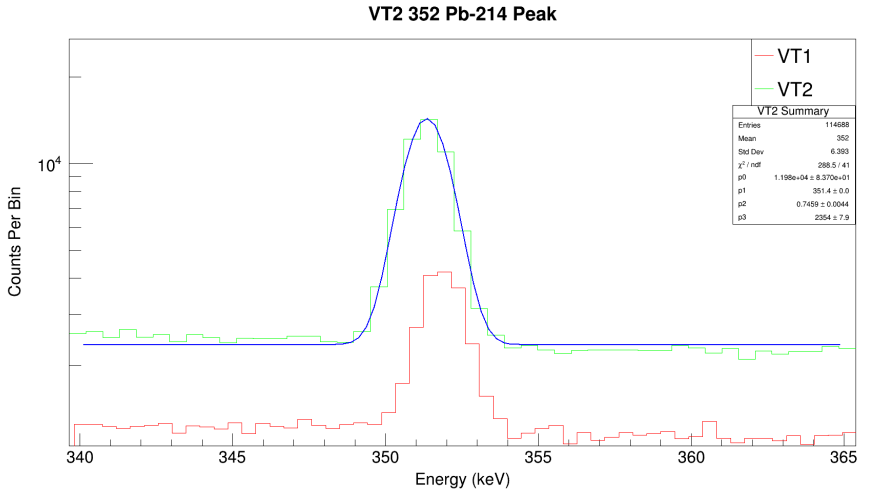

FIG. 22. *VT2's histogram of peak Pb-214 (Lead) with counts per bin on the y-axis and gamma-energies on the x-axis.*

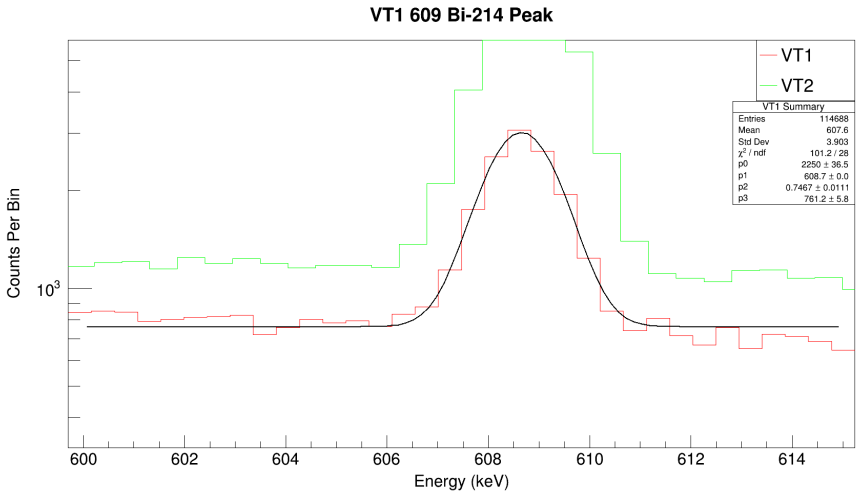

FIG. 23. *VT1's histogram of peak Bi-214 (Bismuth) with counts per bin on the y-axis and gamma-energies on the x-axis.*

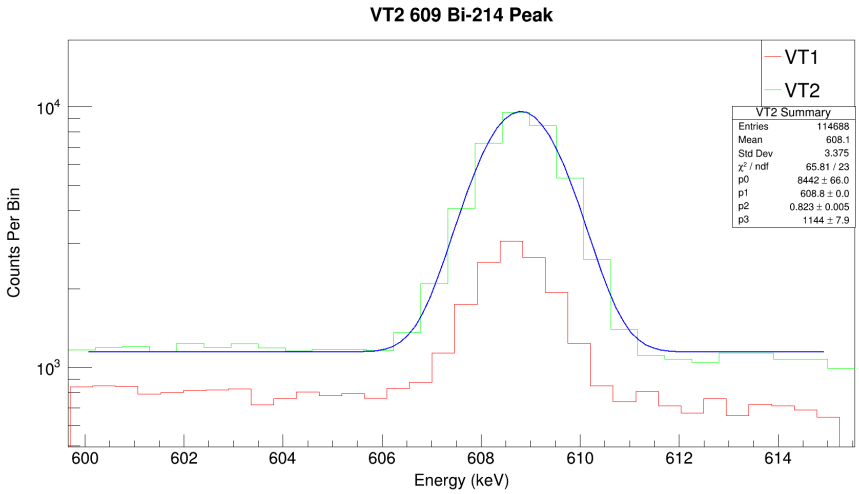

FIG. 24. *VT2's histogram of peak Bi-214 (Bismuth) with counts per bin on the y-axis and gamma-energies on the x-axis.*

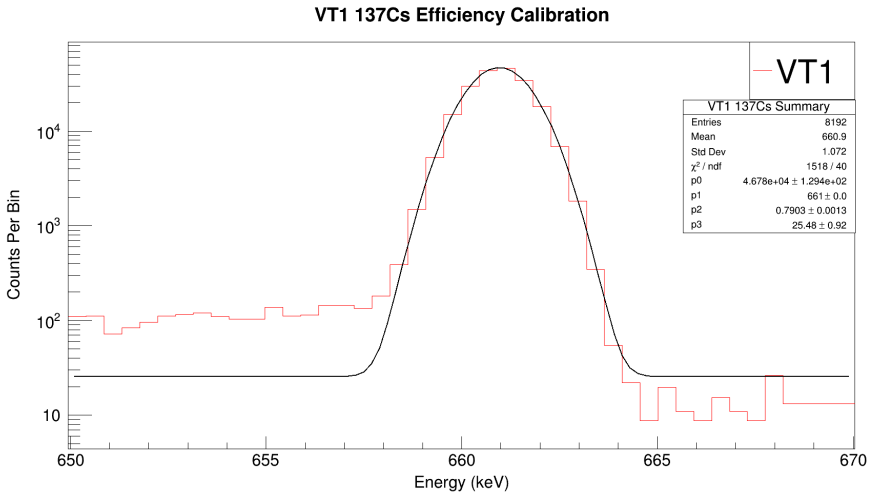

FIG. 25. *Efficiency Calibration histogram for VT1 with a Gaussian curve fitted at the Cs-137(Cesium) 662 keV peak.*

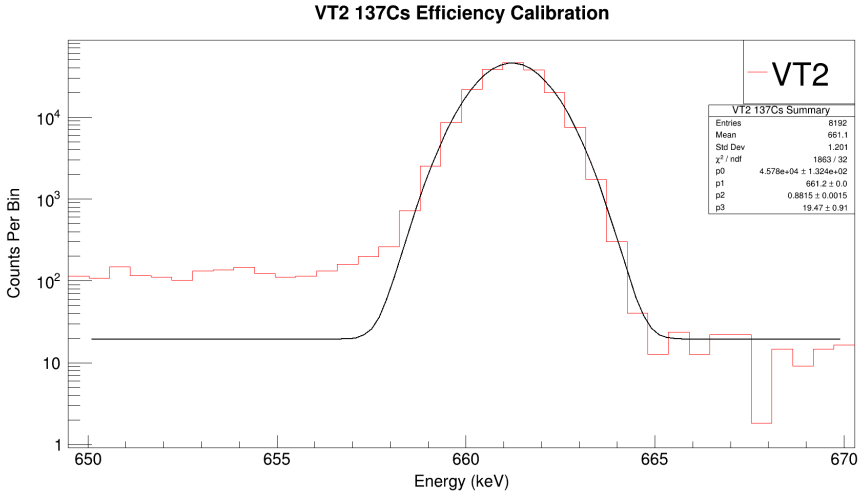

FIG. 26. *Efficiency Calibration histogram for VT2 with a Gaussian curve fitted at the Cs-137(Cesium) 662 keV peak.*

FIG. 27.

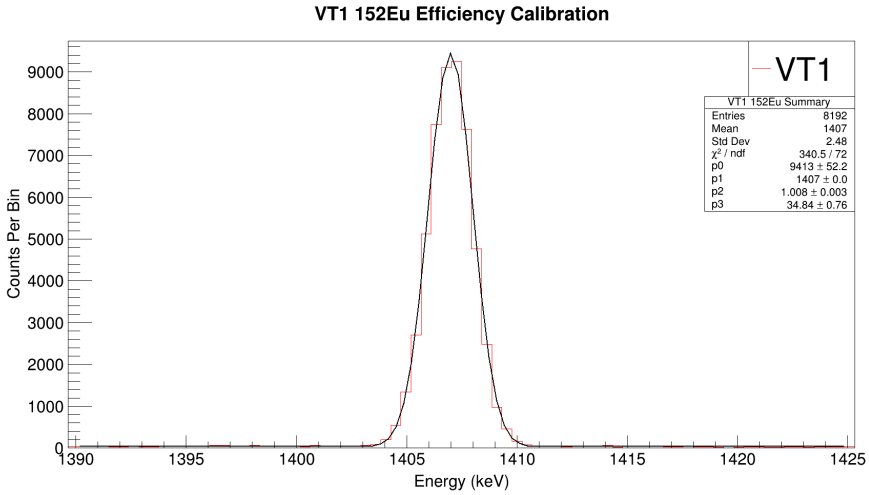

FIG. 28. *Efficiency Calibration histogram for VT1 with a Gaussian curve fitted at the Eu-152(Europium) 1408 keV peak.*

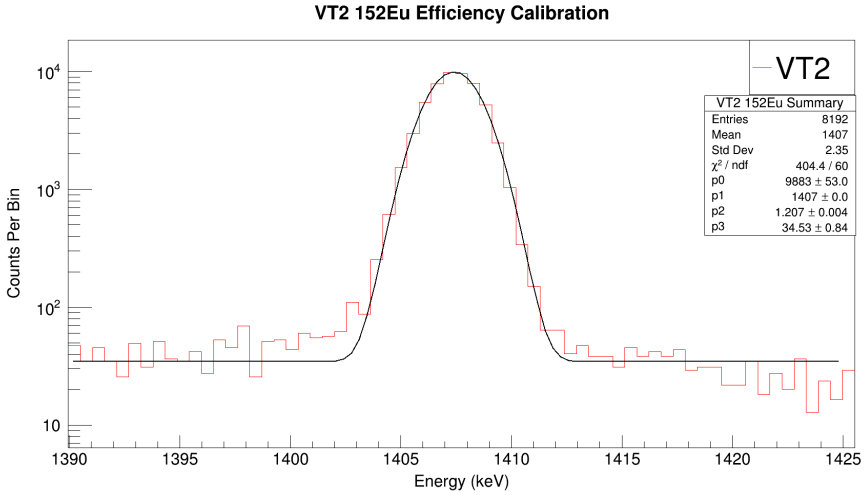

FIG. 29. *Efficiency Calibration histogram for VT2 with a Gaussian curve fitted at the Eu-152(Europium) 1408 keV peak.*

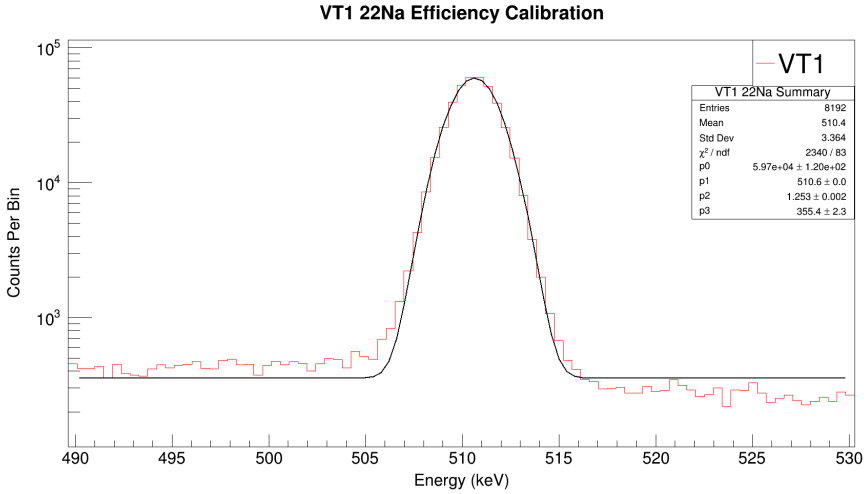

FIG. 30. *Efficiency Calibration histogram for VT1 with a Gaussian curve fitted at the Na-22(Sodium) 510 keV peak.*

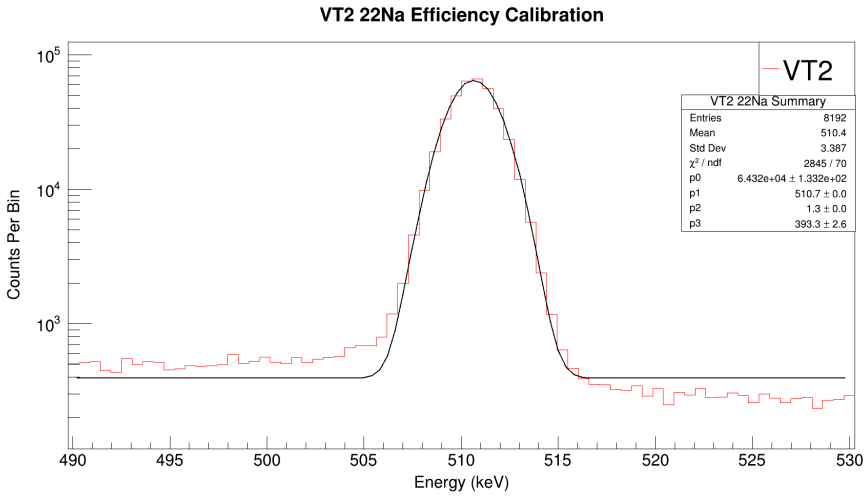

FIG. 31. *Efficiency Calibration histogram for VT2 with a Gaussian curve fitted at the Na-22(Sodium) 510 keV peak.*